EGU 2020: Sharing Geoscience Online
(CR4.1) D2510 | EGU2020-8475

Improving geomorphological process understanding of debris-covered glacier surfaces using aerial robotics

(Miage Glacier, Italian Alps)

Matt Westoby[1*], David Rounce[2], Thomas Shaw[3], Catriona Fyffe[1], Peter Moore[4], Rebecca Stewart[1], Benjamin Brock[1]

[1] Department of Geography and Environmental Sciences, Northumbria University, Newcastle upon Tyne, UK
[2] Geophysical Institute, University of Alaska Fairbanks, Fairbanks, Alaska, USA
[3] Advanced Mining Technology Center, Universidad de Chile, Santiago, Chile
[4] Department of Natural Resource Ecology and Management, Iowa State University, Ames, Iowa, USA

* matt.westoby@northumbria.ac.uk

Rationale:

- There is a need to improve process understanding of debris-covered glacier surface over short timescales because of:
  - (i) rapid, climatically induced areal expansion of debris cover at global scale
  - (i) impacts that debris has on mass balance

- We applied UAV-SfM topographic reconstruction, DEM differencing, and distributed debris thickness modelling to unravel the geomorphological evolution of a 0.15 km^2 region of debris-covered Miage Glacier, Italy, between June 2015 and July 2018 **(Fig. 1)**.

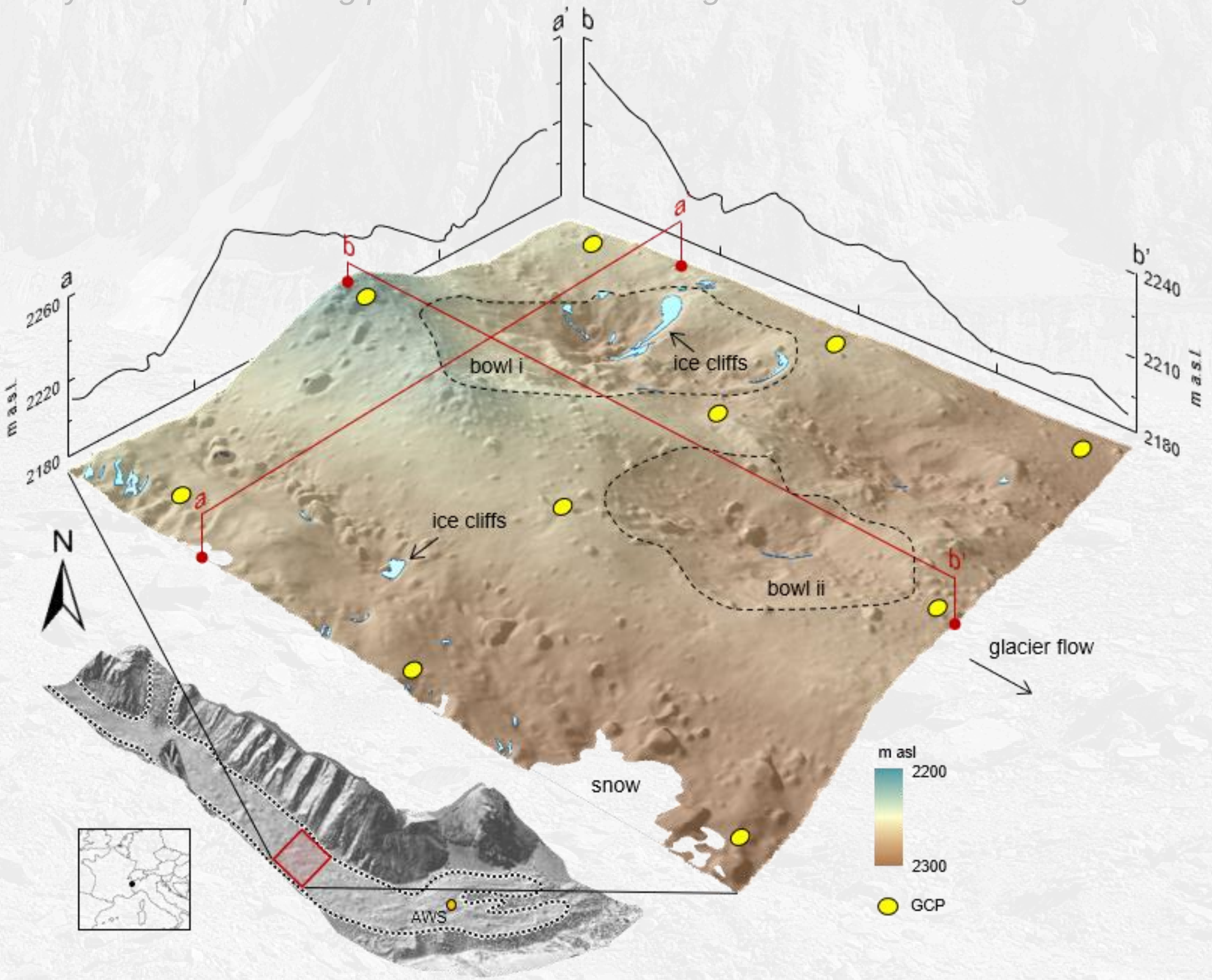

Figure 1. Study site: Glacier du Miage (Miage Glacier), Italian Alps. Main panel is a UAV-SfM-derived DEM. We undertook 4 UAV surveys approx. 1 year apart (July 2015, June 2016, June 2017, June 2018).

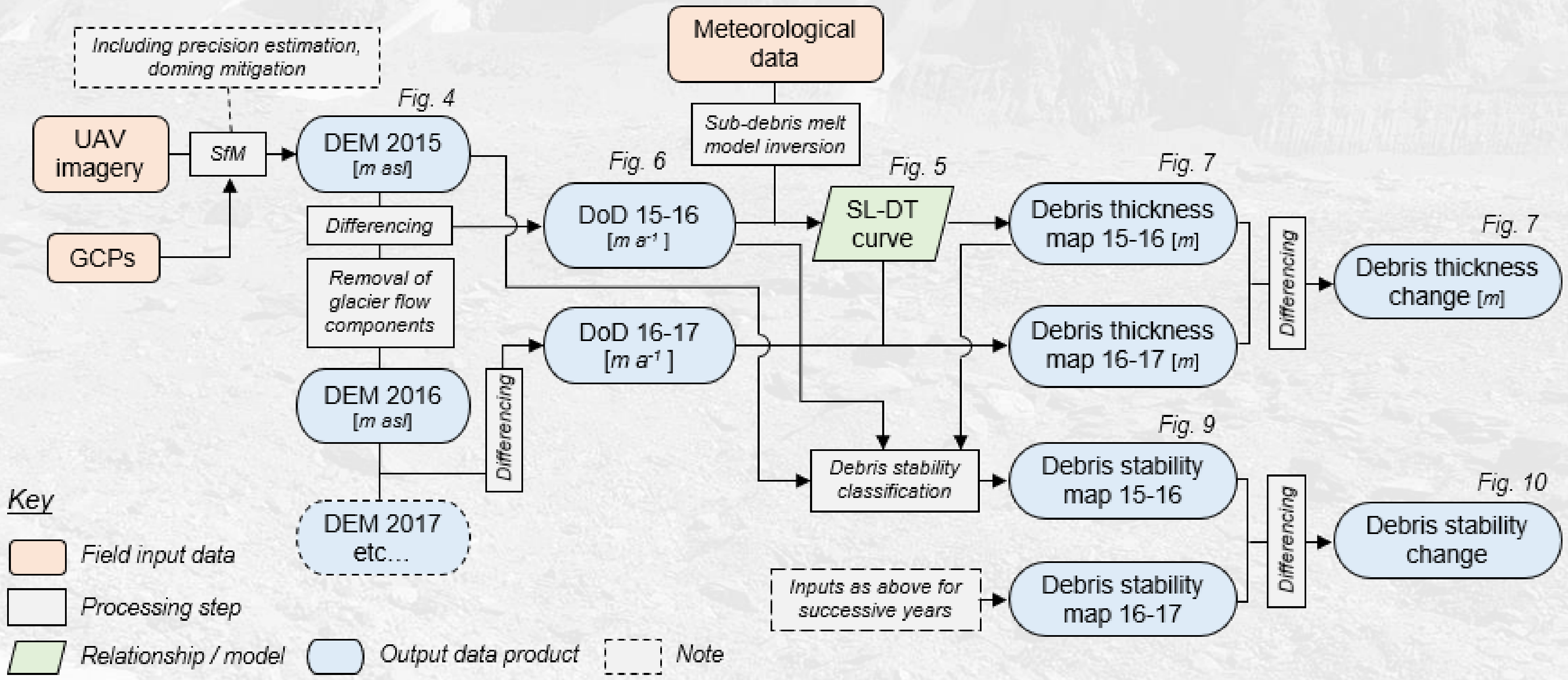

Figure 2. Simplified workflow showing key inputs, outputs and processing steps. Includes cross-references to relevant figures in this presentation.

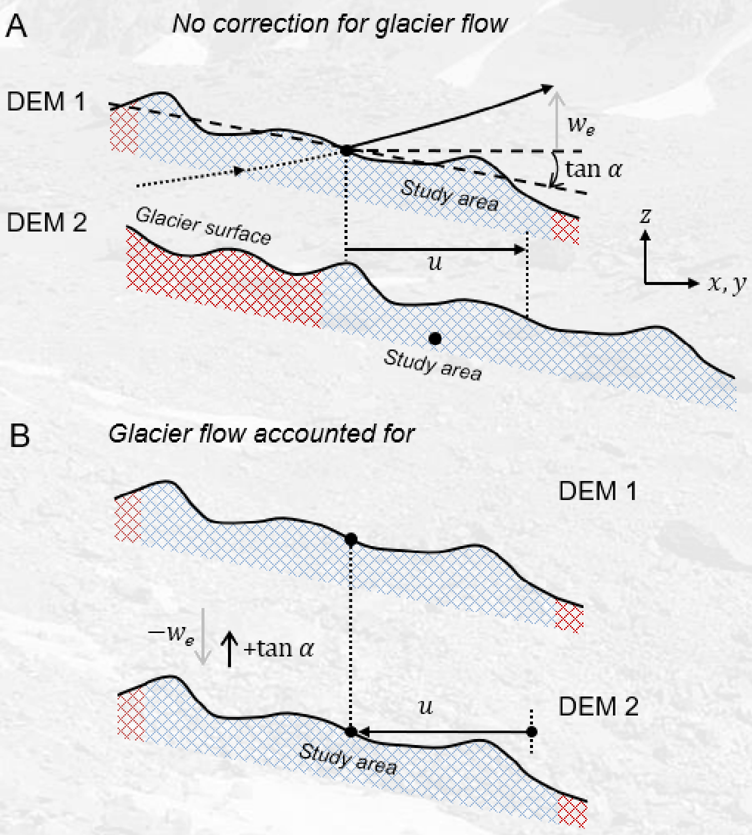

Figure 3. DEM corrections for glacier flow.

DEMs shifted to account for xy displacement (-u) to bring each back in line with earliest (2015) DEM **(Fig. 3)**

DEMs also offset in z to account for valley slope displacement (+tan α) and emergence ($-w_e$) following Vincent et al. (2016), Brun et al. (2018).

The result is a series of flow-corrected DEMs that can be differenced to yield high-res maps of surface lowering **(Fig. 4)**.

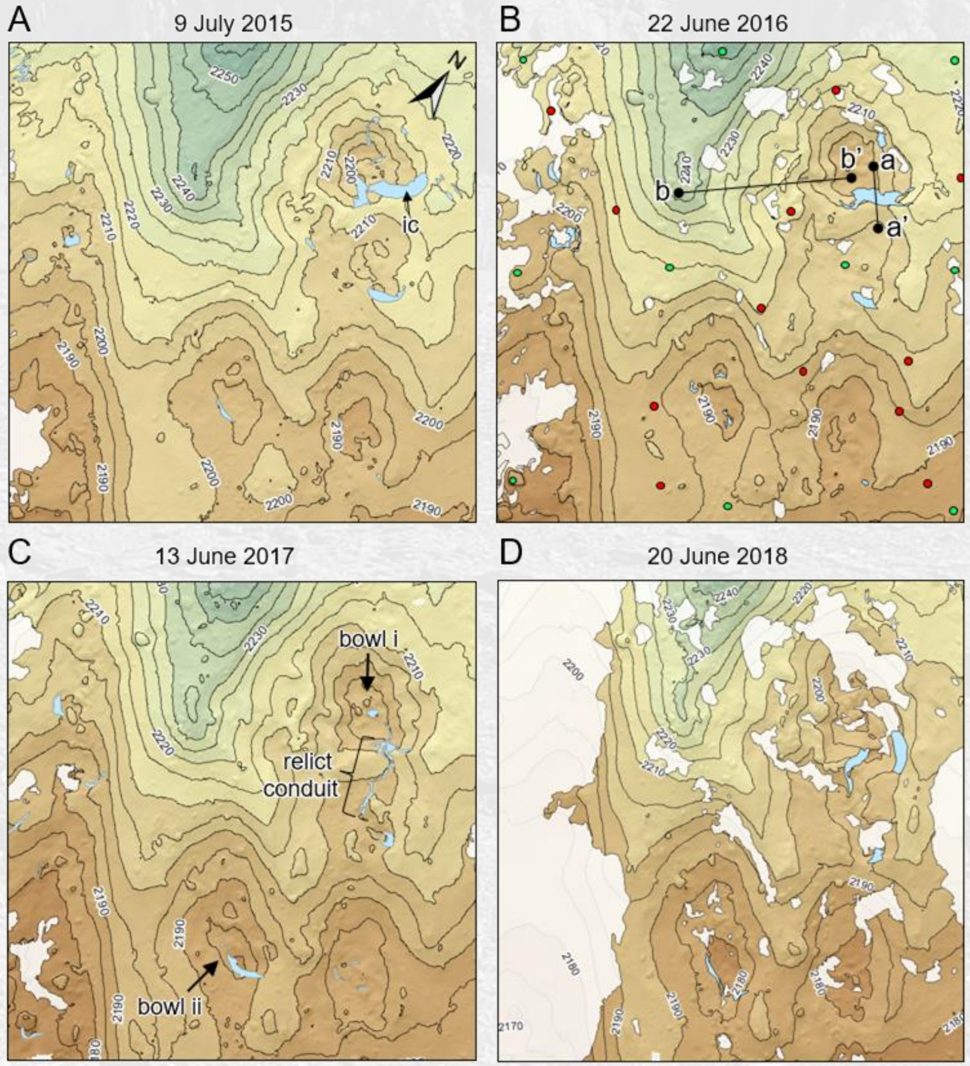

Figure 4. Flow-corrected UAV-SfM-derived DEMs.

- Inverted a sub-debris melt model (Rounce et al., 2018) to produce high spatial resolution (1 m) maps of debris thickness (next slide).
- Model requires: (i) ablation, retrieved from DoDs; (ii) knowledge of debris properties – i.e. albedo, roughness, thermal conductivity – derived from site-specific literature. Model driven using local met data, produces a debris thickness-surface lowering curve.
- Validated model by comparing observed and modelled melt beneath different debris thicknesses using data from Reid and Brock (2010), which represents the most extensive ablation-debris thickness time series for Miage Glacier **(Fig. 5)**.
- Modelled melt agrees well with observations but we do not quantify goodness-of-fit as observations obtained from various positions on the glacier and subject to variations in altitude, aspect, shadowing, etc, which affect local meteorology.

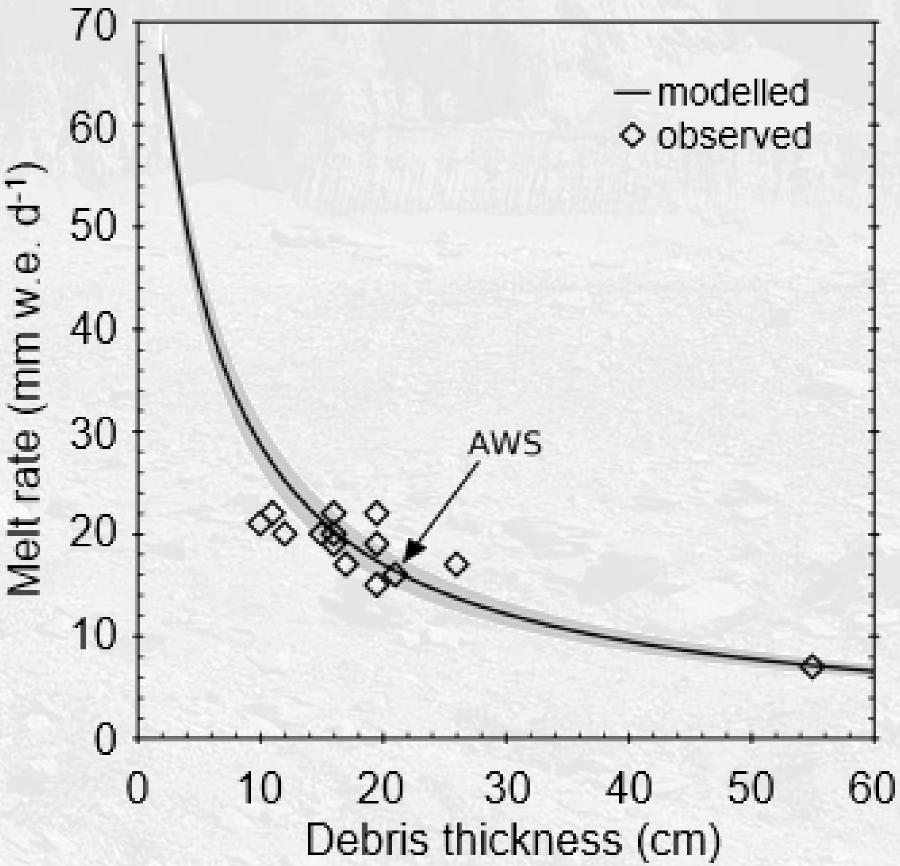

Figure 5. Modelled vs. observed debris thickness-ablation results, including model uncertainty buffer.

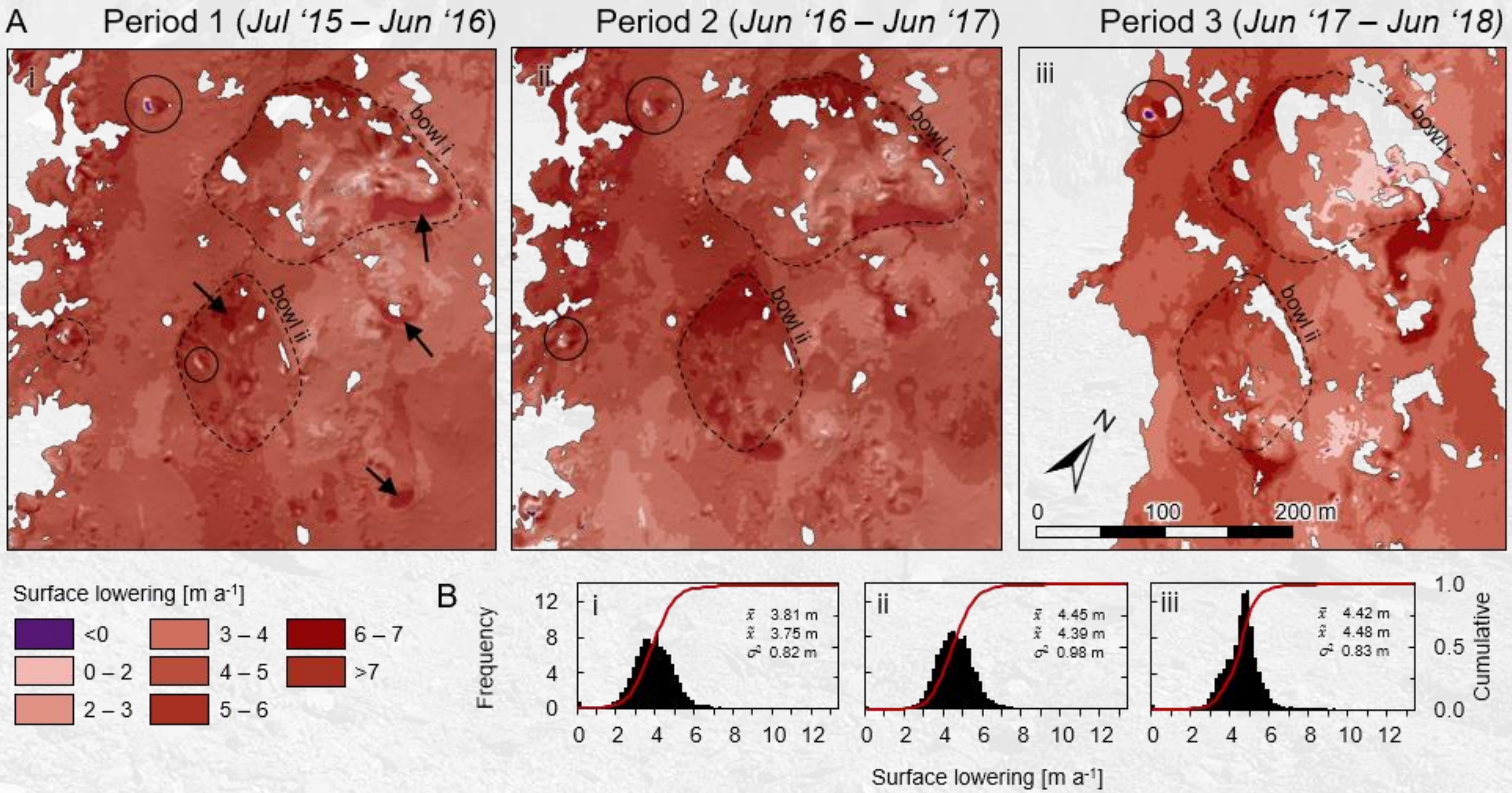

Figure 6. A) DEMs of difference (DoD) showing annual surface lowering. Areas of bare or dirty ice (black arrows) are hotspots of activity in all differencing periods. Mean lowering was 4.49 ± 0.84 m a^{-1}, 4.57 ± 1.10 m a^{-1} and 3.81 ± 1.15 m a^{-1} for periods 1-3, respectively; B) frequency distributions of surface lowering. Black circles in (A) show downslope movement of large boulders.

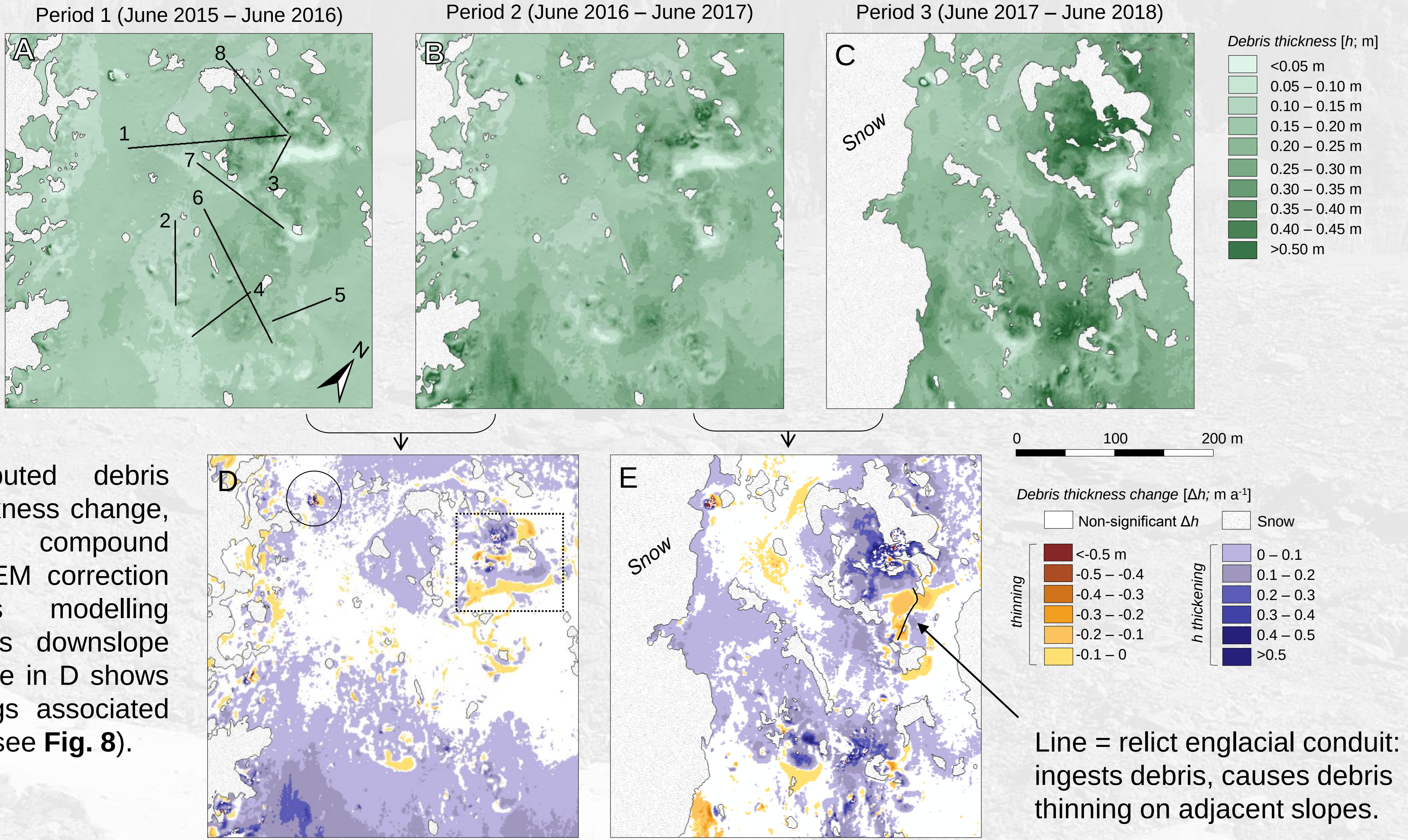

Figure 7. (A) Distributed debris thickness. (B) Debris thickness change, thresholded based on compound uncertainties from the DEM correction and debris thickness modelling workflow. Circle in D is downslope boulder movement. Square in D shows thickening-thinning pairings associated with ice cliff backwasting (see **Fig. 8**).

Lines 1-8 in A = **Fig. 12**)

- **Fig. 8** illustrates fine-scale debris thickening-thinning dynamics in the vicinity of an evolving ice cliff complex.

- We observe corresponding debris thickening-thinning pairings associated with ice cliff backwasting, whereupon debris cascades down the cliff face, leading to localised thinning at the cliff top, and coincident thickening at the cliff toe as a result of this redistribution.

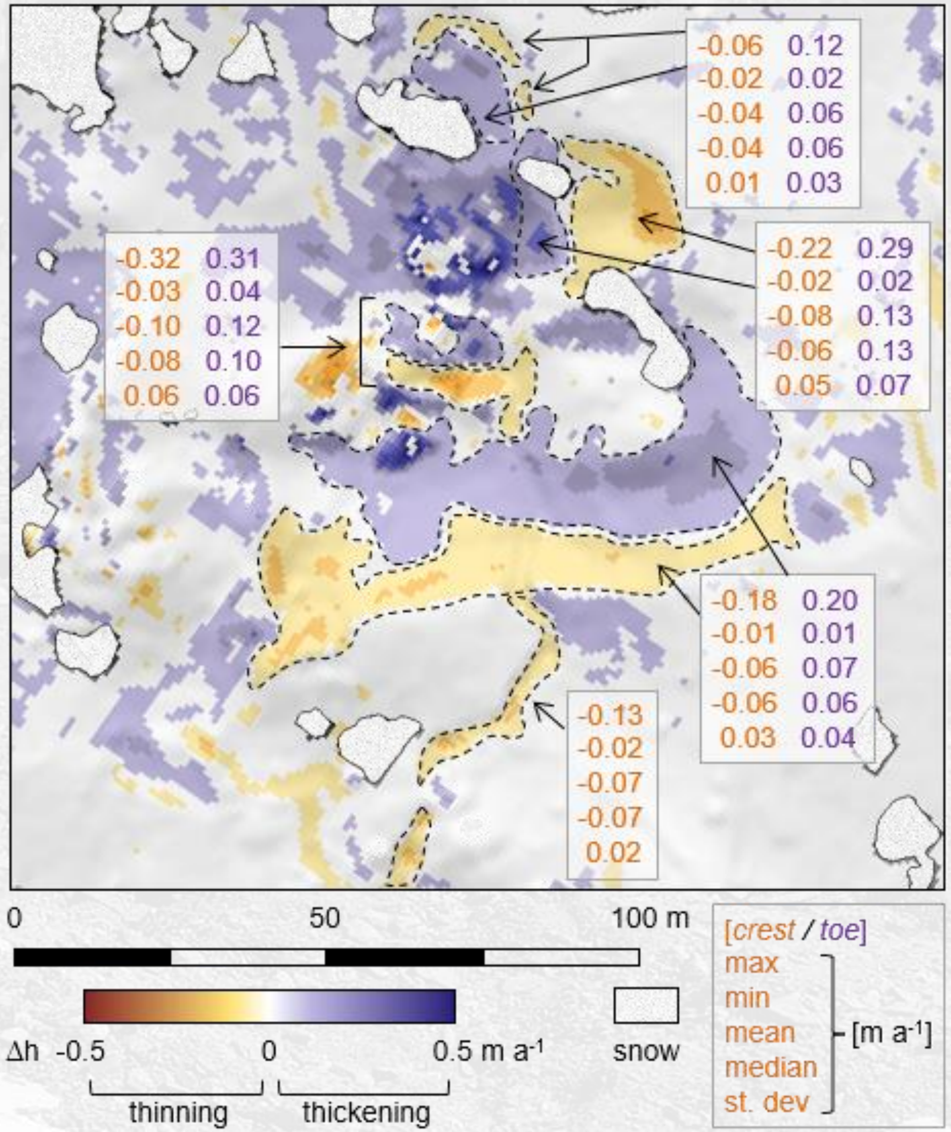

Figure 8. Thresholded debris thickness change between periods 1 and 2.

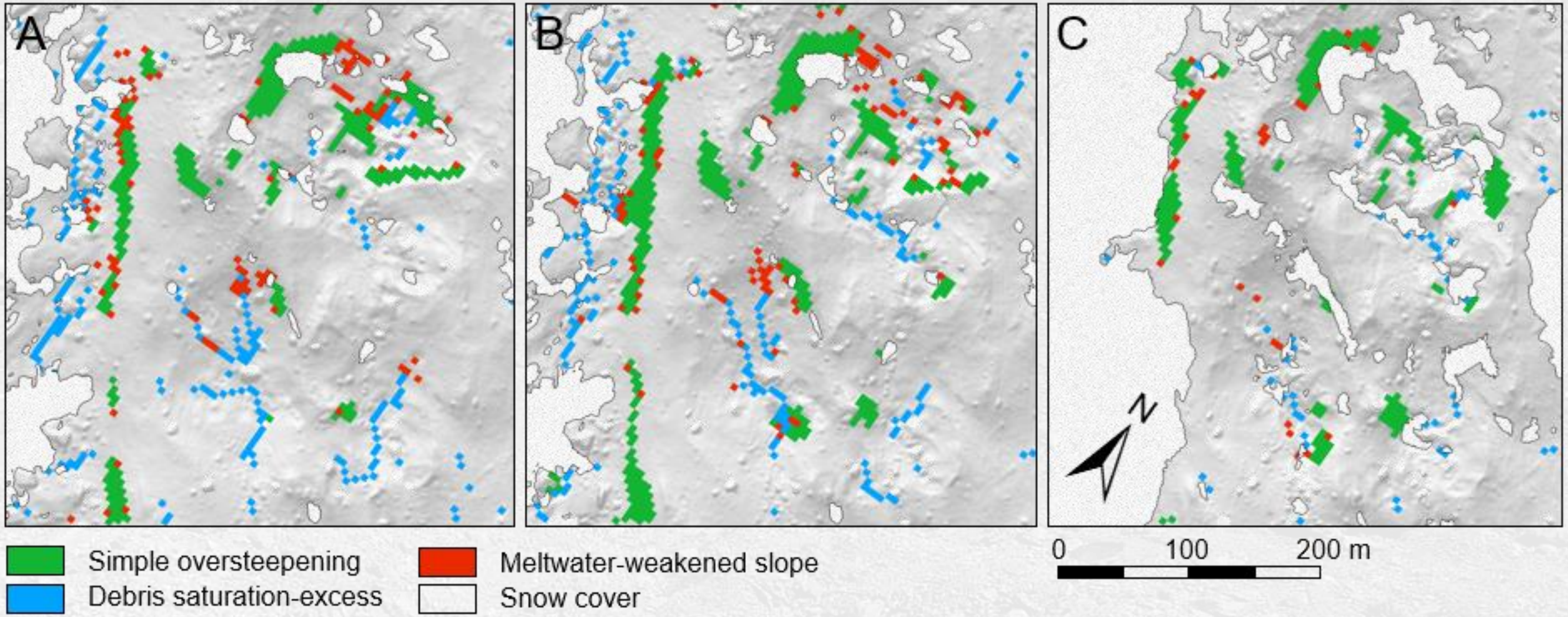

Figure 9. We applied Moore's (2018) method for classifying the (theoretical) debris stability of surface debris, and went on to difference these data (next slide) to quantify spatiotemporal evolution of debris stability. A-C are periods 1-3, respectively.

Figure 10. Spatiotemporal evolution of supraglacial debris stability ⟶

The model predicts the development of ‘newly unstable’ slopes at the margins of unstable terrain – e.g. the top of large backwasting depressions (or ‘bowls’; *black square*).

We model unstable-stable pairings at ice cliffs, which are supported by modelled patterns of debris thickening-thinning (*black rectangle*; **Fig. 8**).

We also model the migration of meltwater-weakened debris instability ‘channels’, which can shift laterally by up to 15 m a^{-1} (*black circle*).

Slopes which become newly unstable are associated with either debris thickening or thinning (median Δh 0.00 m a^{-1}), whilst those which remain stable, stabilise, or remain unstable are associated with net thickening (median Δh +0.06 m a^{-1}).

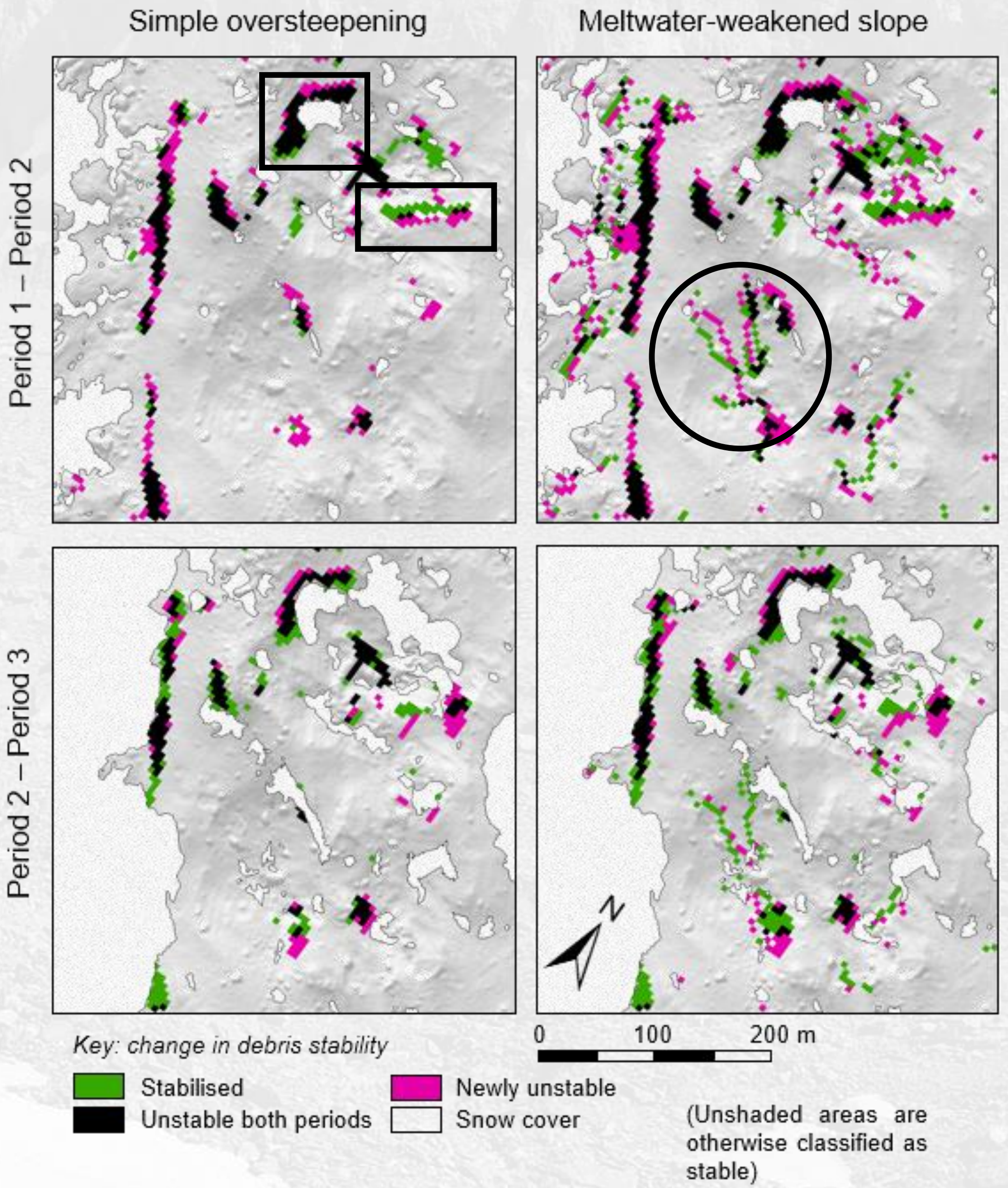

Figure 11. Multi-temporal (A) topographic, (B) ablative, and (C,D) debris thickness evolution along one of the longest continuous slope profiles in the study site.

Significantly, we observe progressive downslope debris layer thickening, and a corresponding increase in the rate of this thickening with distance from the slope crest (D). We attribute this finding to increasing longitudinal buttressing from slope toe deposit as you move downslope, and the capacity for larger clasts to travel further downslope once destabilised, which, combined, lead to an increase in debris thickness with slope-distance.

We attempt to further quantify this effect on the next slide.

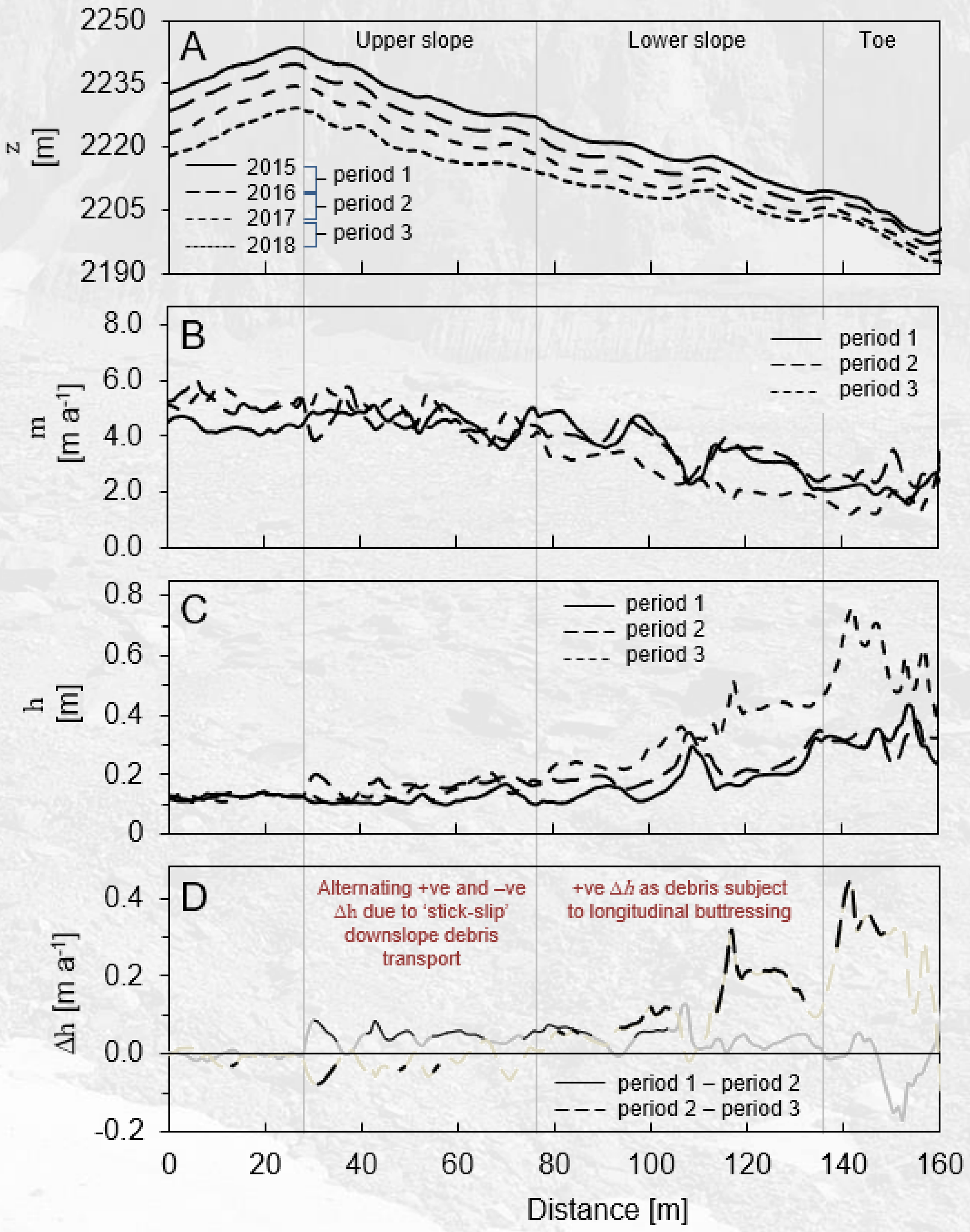

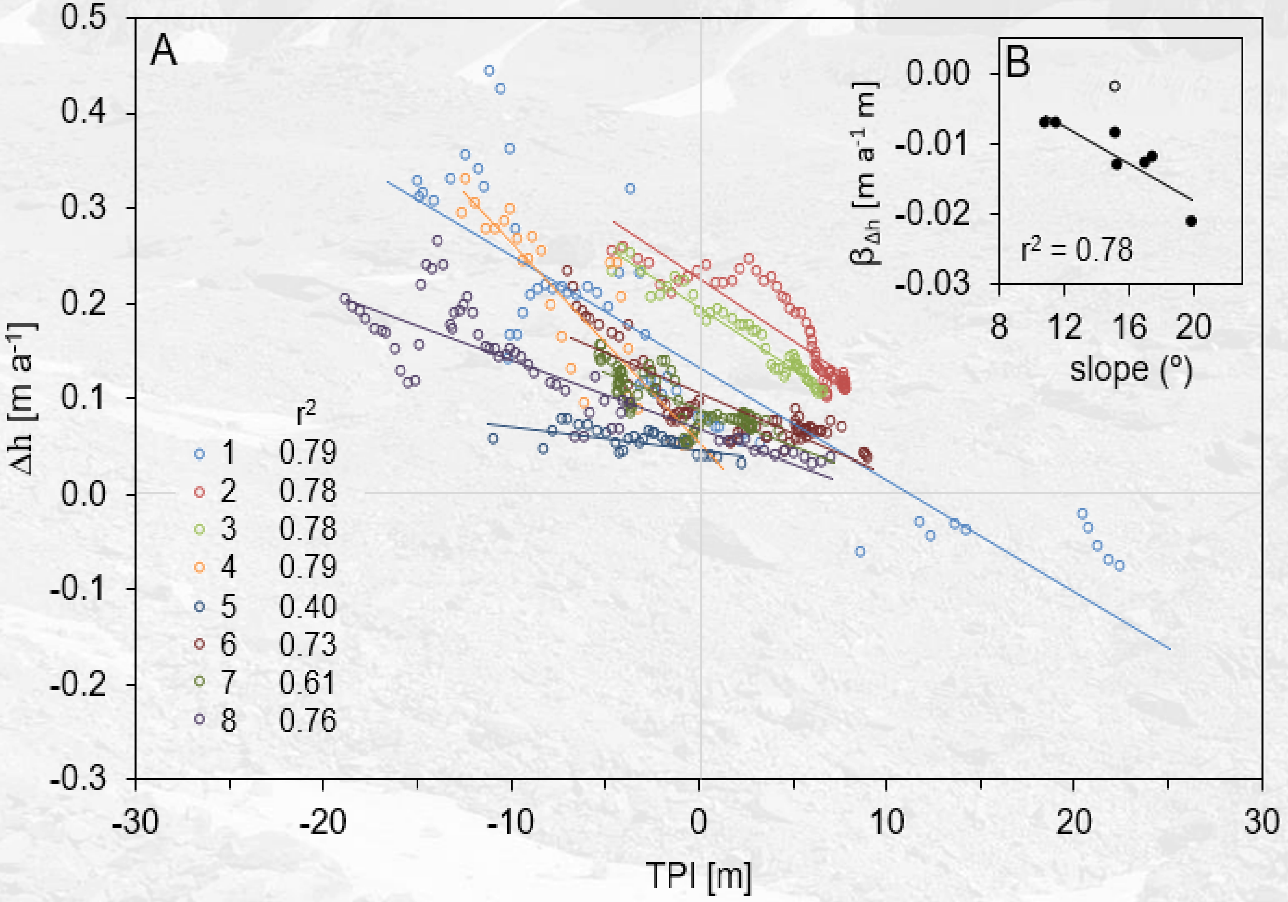

Figure 12. Debris thickness change (Δh) as a function of slope position and angle.

A: Relationships between Δh and the topographic position index (TPI) for all cells along a series of slopes that are representative of the range of slope angles and lengths in the study site. r^2 values for individual slope profiles are inset.

B: Relationship between slope angle (º) and the slope of the linear functions ($\beta_{\Delta h}$) in (A) which describes the rate at which the debris thickness changes with increasing slope-distance. Slope 5 (white marker) is excluded as a statistical outlier.

Take-home finding: the downslope increase in the *rate at which debris cover thickens* can be described as a function of the Topographic Position Index (the normalised elevation of a cell relative to the slope centre), and slope gradient.

Summary:

- Quantifying the evolution of supraglacial topography over short timescales, including debris redistribution, is a challenge. This is partly due to observational limitations, which we can now overcome using repeat high-res topography and the current generation of numerical debris thickness estimation models.

- We applied a multi-method approach to unravel the geomorphological evolution of a region of the Miage Glacier over ~3 year period.

- We observed widespread surface lowering (>3.5 m a^{-1} in all years). Lowering in the vicinity of ice cliffs is far higher (>10 m a^{-1}).

- Debris thickness mapping shows clear thickening-thinning pairings at ice cliffs, supporting their role as efficient agents of debris redistribution.

- The rate at which debris cover thickens can be described as function of topographic position index (TPI) and local slope gradient. Further work is required to test the wider applicability of this relationship, but, tentatively, such models might be useful for forecasting rates and patterns of supraglacial geomorphological development.